

# Effect of grain size, notch width, and testing temperature on the fracture toughness of $\text{Ti}_3\text{Si}(\text{Al})\text{C}_2$ and $\text{Ti}_3\text{AlC}_2$ using the chevron-notched beam (CNB) method

D.T. Wan<sup>a,b</sup>, F.L. Meng<sup>a,b</sup>, Y.C. Zhou<sup>a,\*</sup>, Y.W. Bao<sup>a</sup>, J.X. Chen<sup>a</sup>

<sup>a</sup> Shenyang National Laboratory for Materials Science, Institute of Metal Research, Chinese Academy of Sciences, Shenyang 110016, PR China

<sup>b</sup> Graduate School of Chinese Academy of Sciences, Beijing 100039, PR China

Received 30 March 2007; received in revised form 10 July 2007; accepted 14 July 2007

Available online 12 September 2007

## Abstract

In this work, the effects of grain size, notch width, and testing temperature on the fracture toughness of two typical MAX phases,  $\text{Ti}_3\text{Si}(\text{Al})\text{C}_2$  and  $\text{Ti}_3\text{AlC}_2$ , were investigated using the chevron-notched beam (CNB) method. The high-fracture toughness in the range of 6.43–10.19  $\text{MPa m}^{1/2}$  was determined. The critical notch width is about 250  $\mu\text{m}$  for the valid fracture toughness measurements of  $\text{Ti}_3\text{Si}(\text{Al})\text{C}_2$  and  $\text{Ti}_3\text{AlC}_2$ . For a fixed notch width and testing temperature, the fracture toughness of coarse-grained (CG) samples is higher than that of fine-grained (FG) samples, and the toughness of  $\text{Ti}_3\text{AlC}_2$  is higher than that of  $\text{Ti}_3\text{Si}(\text{Al})\text{C}_2$ . Furthermore, the high-temperature fracture toughness of  $\text{Ti}_3\text{Si}(\text{Al})\text{C}_2$  and  $\text{Ti}_3\text{AlC}_2$  samples show a similar trend that the measured toughness is nearly a constant when the testing temperature is before the ductile–brittle transition temperature (DBTT) and then it declines fast over DBTT. The mechanism for the high-fracture toughness of  $\text{Ti}_3\text{Si}(\text{Al})\text{C}_2$  and  $\text{Ti}_3\text{AlC}_2$  is also discussed.

© 2007 Published by Elsevier Ltd.

**Keywords:** Fracture toughness;  $\text{Ti}_3\text{Si}(\text{Al})\text{C}_2$ ;  $\text{Ti}_3\text{AlC}_2$ ; CNB method; Testing

## 1. Introduction

The fascinating layered ternary ceramics  $\text{M}_{n+1}\text{AX}_n$ , where M is a transition metal, A is IIIA or IVA element, X is C or N, have attracted great attentions from material scientists because they combine the merits of both metals and ceramics.  $\text{Ti}_3\text{SiC}_2$  and  $\text{Ti}_3\text{AlC}_2$  are two typical MAX phases and have been widely investigated by many research groups.<sup>1–15</sup> They possess many salient properties, such as low density, high elastic modulus and strength, easy machinability, good oxidation resistance, excellent thermal shock resistance, and damage tolerance. Fracture toughness is one of the most important parameters related to the reliability of materials and has received much attention because of their basic role in fracture mechanics. As for  $\text{Ti}_3\text{SiC}_2$  and  $\text{Ti}_3\text{AlC}_2$ , many works have been carried out to investigate the

fracture toughness,<sup>6–15</sup> but the  $K_{\text{IC}}$  values are reported to be in a large range from 4.52 to 16  $\text{MPa m}^{1/2}$  for  $\text{Ti}_3\text{SiC}_2$ ,<sup>6–12</sup> and from 4.6 to 9.1  $\text{MPa m}^{1/2}$  for  $\text{Ti}_3\text{AlC}_2$ .<sup>13–15</sup> The discrepancies among these reported  $K_{\text{IC}}$  values mentioned above are probably attributed to the different grain size, the shape and dimension of the sample, sample impurities, different testing methods, and experimental conditions.

Single-edge notched beam (SENB), single-edge pre-cracked beam (SEPB), chevron-notched beam (CNB), indentation strength (IS), indentation fracture (IF), and surface crack in flexure (SCF) testing methods have been developed to determine the fracture toughness of monolithic ceramic.<sup>16–22</sup> Since the indentation crack is hard to induce on the quasi-plastic ceramic,<sup>16</sup> the IS, IF, and SCF methods are unsuitable for  $K_{\text{IC}}$  measurement of the ceramics like  $\text{Ti}_3\text{SiC}_2$  and  $\text{Ti}_3\text{AlC}_2$ . Pre-cracked specimens are difficult to prepare in a reproducible manner, and the initial crack front often cannot be seen on the fracture surface after testing, making it nearly impossible to measure the length of the crack for the SEPB method. For the SENB and CNB methods, notch preparation is critical in the determination of the plane strain fracture toughness

\* Corresponding author at: High-performance Ceramic Division, Shenyang National Laboratory for Materials Science, Institute of Metal Research, Chinese Academy of Sciences, 72 Wenhua Road, Shenyang 110016, PR China.  
Tel.: +86 24 23971765; fax: +86 24 23891320.

E-mail address: [yczhou@imr.ac.cn](mailto:yczhou@imr.ac.cn) (Y.C. Zhou).

$K_{IC}$ . Many works have shown that the notch should be much small (e.g. less than  $66\ \mu\text{m}$  for  $\text{Al}_2\text{O}_3$ )<sup>17</sup> via the SENB method; otherwise, the measured toughness increases with the increment of the notch width.<sup>7,17,18</sup> The fact that a crack develops at the notch tip and extends stably as the load is increased is a unique advantage for the determination of the plane strain fracture toughness by the chevron-notched beam (CNB) method.<sup>19–21</sup> Moreover, the CNB method is an important consideration to evaluate the high-temperature fracture toughness.<sup>17,22</sup> Due to the apparent advantages, the CNB method was widely used<sup>17,19–22</sup> and was recognized as a standard method to measure the fracture toughness of ceramic materials.<sup>23</sup> However, few attempts to determine the fracture toughness of MAX phases using the CNB method can be found in the literature.

It is worth noting that all of the testing specimens of  $\text{Ti}_3\text{SiC}_2$  mentioned above contain some impurities like TiC and/or  $\text{TiSi}_2$ ,<sup>6–12</sup> which will inevitably influence the measured toughness of  $\text{Ti}_3\text{SiC}_2$ . To eliminate the ill effect of the impurities on the toughness of  $\text{Ti}_3\text{SiC}_2$ , TiC-free  $\text{Ti}_3\text{Si}(\text{Al})\text{C}_2$  was used as one species of the testing samples. Since  $\text{Ti}_3\text{Si}(\text{Al})\text{C}_2$  and  $\text{Ti}_3\text{AlC}_2$  is a promising structure component at high temperatures,<sup>24–26</sup> understanding the temperature dependence of mechanical properties including fracture toughness is helpful for the design and application of these two ceramics. Hence, it is strongly needed to determine the fracture toughness of  $\text{Ti}_3\text{Si}(\text{Al})\text{C}_2$  and  $\text{Ti}_3\text{AlC}_2$  at both room and high temperatures.

In this work, specimens of  $\text{Ti}_3\text{Si}(\text{Al})\text{C}_2$  and  $\text{Ti}_3\text{AlC}_2$  with two different grain sizes, named fine-grained (FG) and coarse-grained (CG) samples, were prepared by hot pressing (HP) method and used to measure the fracture toughness using the CNB method. The effects of notch width and testing temperature were also investigated. The results will be beneficial for the promotion of  $\text{Ti}_3\text{Si}(\text{Al})\text{C}_2$  and  $\text{Ti}_3\text{AlC}_2$  as candidates for structural materials and for the understanding of the intrinsic fracture resistance of  $\text{Ti}_3\text{Si}(\text{Al})\text{C}_2$  and  $\text{Ti}_3\text{AlC}_2$  materials.

## 2. Experimental procedure

Bulk  $\text{Ti}_3\text{Si}(\text{Al})\text{C}_2$  and  $\text{Ti}_3\text{AlC}_2$  materials with different grain sizes were fabricated by the in situ hot pressing/solid–liquid reaction synthesis, which was also described elsewhere.<sup>14,27</sup> The true phase composition of  $\text{Ti}_3\text{Si}(\text{Al})\text{C}_2$  is  $\text{Ti}_3\text{Si}_{0.95}\text{Al}_{0.05}\text{C}_2$ . Briefly, the elemental powders of Ti (99%, –300 mesh), Si (99.5%, –300 mesh), Al (99%, –200 mesh), and graphite (98%, –200 mesh) were used as the initial materials and precisely weighed according to the target composition, and then mixed in an agate mill for 15 h in a wet medium. After milling and drying, the mixtures were screened through a 60-mesh sieve and cold compacted into a  $\varnothing\ 50\ \text{mm}$  graphite mold coated with boron nitride (BN). To obtain the FG samples, the green compacts were hot-pressed at 30 MPa under a flowing Ar atmosphere at 1550 °C for 60 min, and subsequently annealed at 1400 °C for 30 min for FG  $\text{Ti}_3\text{Si}(\text{Al})\text{C}_2$ , and at 1520 °C for 30 min for FG  $\text{Ti}_3\text{AlC}_2$ . To get the CG specimens, the green compacts were hot-pressed at 30 MPa under a flowing Ar

atmosphere at 1620 °C for 60 min and subsequently annealed at 1470 °C for 30 min for CG  $\text{Ti}_3\text{Si}(\text{Al})\text{C}_2$ , and at 1520 °C for 30 min and further annealed at 1580 °C for 120 min for CG  $\text{Ti}_3\text{AlC}_2$ .

The densities of the as-prepared materials were determined by Archimedes's method. The phase compositions were identified by X-ray diffraction (XRD) using powders drilled from the bulk samples. The XRD data were collected by a step-scanning diffractometer with Cu  $K\alpha$  radiation (Rigaku D/max-2400, Tokyo, Japan). The microstructure of the materials was examined in a SUPRA 35 scanning electron microscope (SEM) (LEO, Oberkochen, Germany) equipped with an energy-dispersive spectroscopy (EDS) system. To expose the  $\text{Ti}_3\text{Si}(\text{Al})\text{C}_2$  and  $\text{Ti}_3\text{AlC}_2$  grain, samples were mechanically polished up to 1200# SiC paper and etched by a  $\text{HNO}_3\text{:HF:H}_2\text{O}$  (1:1:2) solution before SEM observation. The Vickers hardness was tested on the polished surfaces at 9.80 N with a dwell time of 15 s. The dynamic elastic moduli of  $\text{Ti}_3\text{Si}(\text{Al})\text{C}_2$  and  $\text{Ti}_3\text{AlC}_2$  samples at room temperature were measured in a RFDA-HTVP1750-C testing machine (IMCE, Diepenbeek, Belgium).<sup>26</sup> The specimens for flexural strength were rectangular bars of  $3\ \text{mm} \times 4\ \text{mm} \times 36\ \text{mm}$  in size. Three-point bending tests with a crosshead speed of 0.5 mm/min were performed to measure the flexural strength of  $\text{Ti}_3\text{Si}(\text{Al})\text{C}_2$  and  $\text{Ti}_3\text{AlC}_2$ .

Specimens with dimensions of  $3\ \text{mm} \times 4\ \text{mm} \times 36\ \text{mm}$  were electrical-discharge machined from the as-prepared bulk  $\text{Ti}_3\text{Si}(\text{Al})\text{C}_2$  and  $\text{Ti}_3\text{AlC}_2$ . Chevron notches were introduced by diamond-coated wheel slotting. To study the effect of the notch width on the fracture toughness, four types of blade with the thickness of 0.054, 0.117, 0.169, and 0.365 mm, respectively, were used to introduce the chevron notches. After that, the true notch width was measured by optical microscope (OM). Four-point bending tests with a crosshead speed of 0.05 mm/min were performed for fracture toughness measurements and then the fractured surfaces were examined by means of SEM and OM. To investigate the effect of testing temperature, the fracture toughness of  $\text{Ti}_3\text{Si}(\text{Al})\text{C}_2$  and  $\text{Ti}_3\text{AlC}_2$  was measured at various temperatures from room temperature up to 1200 °C. The fixtures for high-temperature tests were made of  $\alpha\text{-SiC}$ . The testing specimens were heated to the target temperatures with a heating rate of 10 °C/min. Prior to the tests, all the samples were held for 20 min to make sure the temperature equilibrium. No attempt was made to avoid the oxidation of the samples during the tests at high temperatures. For each condition, three to five specimens were tested to ensure the veracity. The fracture toughness measured with the four-point bending tests using CNB specimens was calculated using the equation,<sup>21,23</sup>

$$K_{IC} = \frac{P(S_o - S_i)}{BW^{3/2}} \times Y_{\min}^* \quad (1)$$

where  $P$  is the critical load,  $S_o$  the outer span (30 mm),  $S_i$  the inner span (10 mm),  $B$  the width of sample,  $W$  the thickness of the sample,  $Y_{\min}^*$  the stress intensity factor coefficient for the

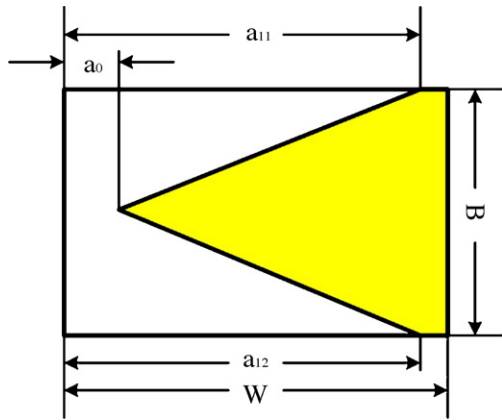


Fig. 1. Schematic illustration of the model for the chevron notch beam (CNB) method.

CNB method and given in,<sup>21,23</sup>

$$Y_{\min}^* = \left[ 2.92 + 4.52 \left( \frac{a_0}{W} \right) + 10.14 \left( \frac{a_0}{W} \right)^2 \right] \times \sqrt{\frac{(a_1/W) - (a_0/W)}{1.0 - (a_0/W)}} \quad (2)$$

where  $a_0$  is the distance from the chevron tip to the specimen surface at the notch mouth (the tensile surface),  $a_1$  the average

notched depths on the two side surfaces ( $a_1 = (a_{11} + a_{12})/2$ ), as shown in Fig. 1.

### 3. Results

#### 3.1. Phase composition, microstructure, and mechanical properties

The samples prepared by the in situ hot pressing method were fully dense (98–99% of the theoretical density). The XRD analysis shown in Fig. 2 reveals that no impurities like TiC or TiSi<sub>2</sub> are detected in Ti<sub>3</sub>Si(Al)C<sub>2</sub> and no TiC is found in FG Ti<sub>3</sub>AlC<sub>2</sub>, while a small amount of TiC (about 7 vol.%) is found in the CG Ti<sub>3</sub>AlC<sub>2</sub>. Fig. 3 compares the etched surface of FG Ti<sub>3</sub>Si(Al)C<sub>2</sub> (Fig. 2(a)), CG Ti<sub>3</sub>Si(Al)C<sub>2</sub> (Fig. 2(b)), FG Ti<sub>3</sub>AlC<sub>2</sub> (Fig. 2(c)), and CG Ti<sub>3</sub>AlC<sub>2</sub> (Fig. 2(d)) samples. The large elongated Ti<sub>3</sub>Si(Al)C<sub>2</sub> grains show layered characteristics and their longitudinal edges are parallel to (0001) planes of Ti<sub>3</sub>SiC<sub>2</sub>.<sup>28</sup> It can be found that the grain length and grain width of the CG samples are  $48.7 \pm 41.2$  and  $15.4 \pm 11.7$  μm for Ti<sub>3</sub>Si(Al)C<sub>2</sub>, respectively, which is about three times higher than those of the FG Ti<sub>3</sub>Si(Al)C<sub>2</sub> samples. For Ti<sub>3</sub>AlC<sub>2</sub>, the grain length and grain width of the CG samples are  $74.9 \pm 23.4$  and  $19.1 \pm 8.1$  μm, which is in excess four times than those of the FG Ti<sub>3</sub>AlC<sub>2</sub> specimens.

The physical and mechanical properties of the Ti<sub>3</sub>Si(Al)C<sub>2</sub> and Ti<sub>3</sub>AlC<sub>2</sub> were summarized in Table 1. It can be seen that

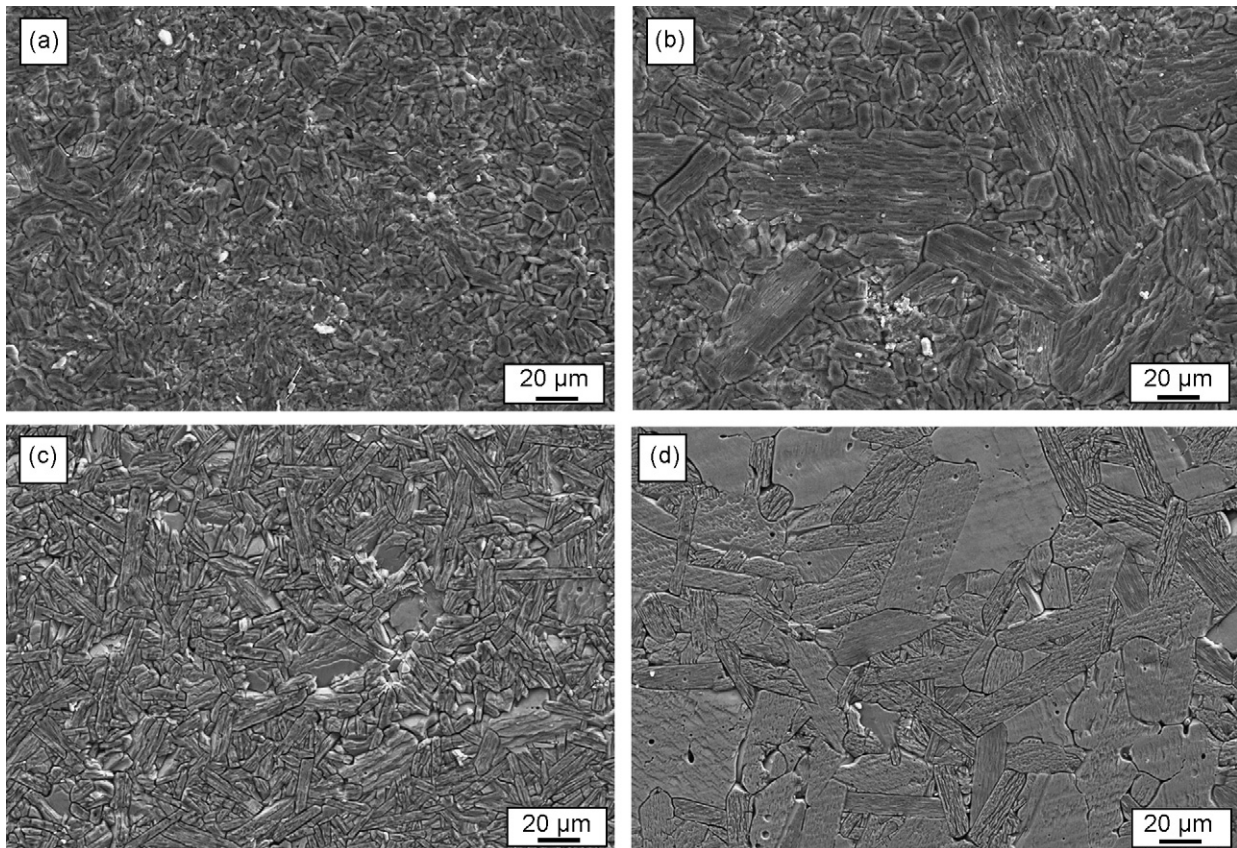


Fig. 2. Typical micrographs of the etched fracture surface for FG Ti<sub>3</sub>Si(Al)C<sub>2</sub> (a), CG Ti<sub>3</sub>Si(Al)C<sub>2</sub> (b), FG Ti<sub>3</sub>AlC<sub>2</sub> (c), and CG Ti<sub>3</sub>AlC<sub>2</sub> (d) samples.



Table 1  
Physical and mechanical properties of FG  $\text{Ti}_3\text{Si}(\text{Al})\text{C}_2$ , CG  $\text{Ti}_3\text{Si}(\text{Al})\text{C}_2$ , FG  $\text{Ti}_3\text{AlC}_2$ , and CG  $\text{Ti}_3\text{AlC}_2$  samples

Properties	FG $\text{Ti}_3\text{Si}(\text{Al})\text{C}_2$	CG $\text{Ti}_3\text{Si}(\text{Al})\text{C}_2$	FG $\text{Ti}_3\text{AlC}_2$	CG $\text{Ti}_3\text{AlC}_2$
Density ( $\text{g}/\text{cm}^3$ )	4.47 (98.9%)	4.46 (98.7%)	4.20 (98.9%)	4.19 (98.6%)
Grain width ( $\mu\text{m}$ )	$4.2 \pm 1.4$	$16.1 \pm 9.3$	$6.5 \pm 2.1$	$19.1 \pm 8.1$
Grain length ( $\mu\text{m}$ )	$15.4 \pm 11.7$	$48.7 \pm 41.2$	$28.4 \pm 9.5$	$74.9 \pm 23.4$
Elastic modulus (GPa)	336	335	304	301
Vickers hardness (GPa)	$4.02 \pm 0.12$	$3.28 \pm 0.17$	$3.46 \pm 0.16$	$2.22 \pm 0.22$
Flexural strength (MPa)	$458.5 \pm 25.8$	$306.4 \pm 13.6$	$320.3 \pm 11.2$	$169.2 \pm 12.9$

the grain size has little effect on the dynamic elastic modulus, but has great influence on the measured flexural strength and Vickers hardness. For  $\text{Ti}_3\text{Si}(\text{Al})\text{C}_2$ , the flexural strength and Vickers hardness of CG samples are  $306.4 \pm 13.6$  MPa and  $3.28 \pm 0.17$  GPa, respectively. Compared with that of the FG samples, the strength and hardness decrease by about 33.2 and 18.4%. For  $\text{Ti}_3\text{AlC}_2$ , the strength and hardness of CG specimens are  $169.2 \pm 12.9$  MPa and  $2.22 \pm 0.22$  GPa. Compared with that of the FG samples, the strength and hardness decrease by about 47.2 and 35.8%, respectively.

### 3.2. Fracture toughness determined by CNB method

Fig. 3 shows the typical optical micrograph of the testing specimen with the chevron notch prepared by the diamond-coated blade with the thickness of 0.054 mm, which indicates that a successful chevron notch is introduced. Fig. 4 represents the measured fracture toughness of  $\text{Ti}_3\text{Si}(\text{Al})\text{C}_2$  and  $\text{Ti}_3\text{AlC}_2$  as a function of the true notch width. High fracture toughness of  $6.4\text{--}9.5$   $\text{MPa m}^{1/2}$  for this kind of ceramics (MAX phases) is found. It can also be seen that the fracture toughness of  $\text{Ti}_3\text{AlC}_2$  is higher than that of  $\text{Ti}_3\text{Si}(\text{Al})\text{C}_2$ , and the toughness of CG samples is slightly higher than those of FG samples for both  $\text{Ti}_3\text{Si}(\text{Al})\text{C}_2$  and  $\text{Ti}_3\text{AlC}_2$ . For the FG and CG samples, the scatter of the standard deviation is rather limited when the notch width is less than  $250$   $\mu\text{m}$ , whereas it becomes quite large when the notch width is  $383$   $\mu\text{m}$ . To check the stability of crack propagation, the typical curves of the force as a function of testing time for different notch width is shown in Fig. 5. For CG and

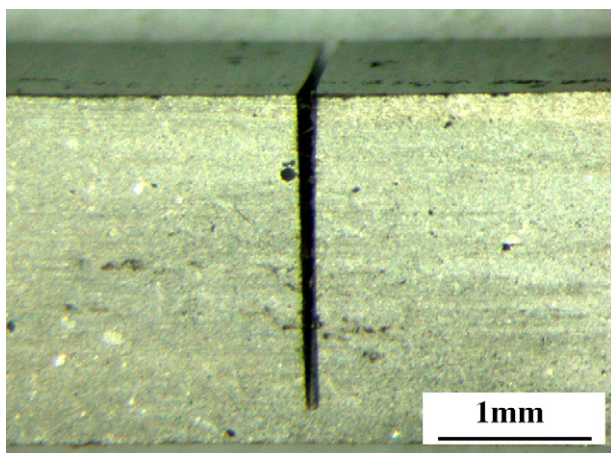


Fig. 3. Optical micrograph of the typical testing samples for CNB method. The notch was introduced by a 0.057 mm blade diamond saw.

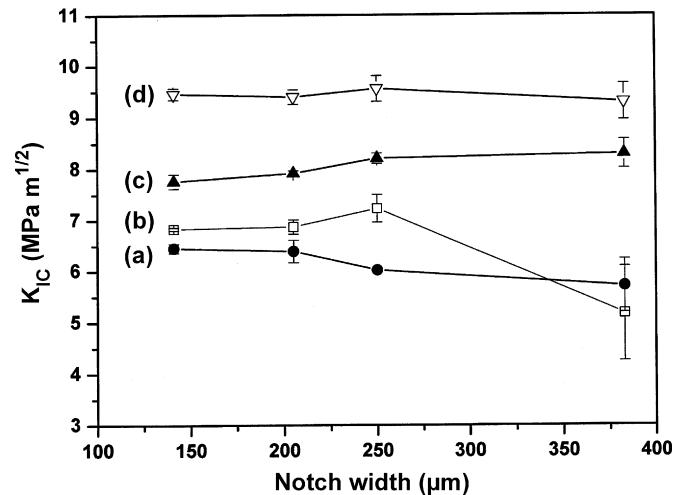


Fig. 4. The measured fracture toughness of FG  $\text{Ti}_3\text{Si}(\text{Al})\text{C}_2$  (a), CG  $\text{Ti}_3\text{Si}(\text{Al})\text{C}_2$  (b), FG  $\text{Ti}_3\text{AlC}_2$  (c), and CG  $\text{Ti}_3\text{AlC}_2$  (d) samples as a function of the true notch width.

FG samples of  $\text{Ti}_3\text{Si}(\text{Al})\text{C}_2$  and  $\text{Ti}_3\text{AlC}_2$  with the notch width less than  $250$   $\mu\text{m}$ , the test force–time records exhibit a smooth, nonlinear transition to the maximum force prior to final fracture, which confirms that the test is stable.<sup>29</sup> When the notch width is about  $383$   $\mu\text{m}$ , the test is becoming unstable. For  $\text{Ti}_3\text{Si}(\text{Al})\text{C}_2$  and  $\text{Ti}_3\text{AlC}_2$ , the crack propagation will convert from stable to unstable, which agrees well with the results in Fig. 4. Hence, the critical notch width of  $250$   $\mu\text{m}$  is recommended for  $K_{IC}$

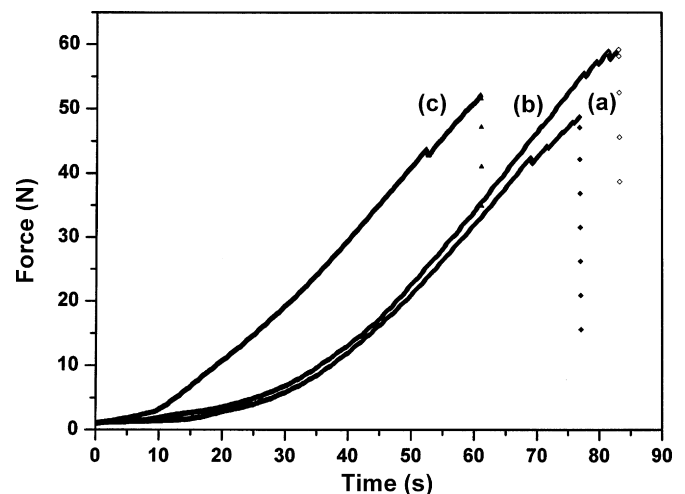


Fig. 5. The force as a function of testing time during the loading for  $\text{Ti}_3\text{Si}(\text{Al})\text{C}_2$  with the notch width of  $141$  (a),  $250$  (b), and  $383$   $\mu\text{m}$  (c).

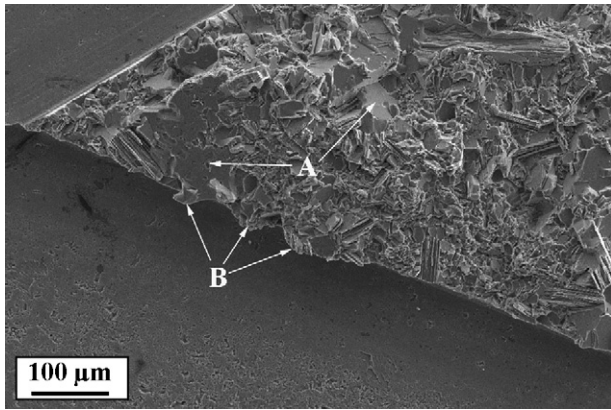


Fig. 6. Typical fracture surface of  $\text{Ti}_3\text{Si}(\text{Al})\text{C}_2$  with the notch less than  $250\ \mu\text{m}$ , showing the intrinsic fracture resistance. “A” showing basal plane slip; “B” showing pull-out of the grains.

calculation of  $\text{Ti}_3\text{Si}(\text{Al})\text{C}_2$  and  $\text{Ti}_3\text{AlC}_2$ . Fig. 6 displays the typical fracture surface of the testing specimens with the notch width less than  $250\ \mu\text{m}$  after bending. It can be found that intergranular fracture is dominant at the apex of the triangular ligament and that transgranular fracture occurs frequently in the latter part near to the tail of the chevron notch. The delamination and pull-out of the laminated grains are also found in Fig. 6, which may be dominant in the energy absorbing mechanism.

To investigate the effect of testing temperature on the fracture toughness of  $\text{Ti}_3\text{Si}(\text{Al})\text{C}_2$  and  $\text{Ti}_3\text{AlC}_2$ , the notch width was chosen to be a fixed value of  $141\ \mu\text{m}$ . Fig. 7 shows the fracture toughness of the CG and FG samples of  $\text{Ti}_3\text{Si}(\text{Al})\text{C}_2$  and  $\text{Ti}_3\text{AlC}_2$  as a function of the testing temperature. For all the testing temperatures, the fracture toughness of CG specimens is higher than that of FG samples. The fracture toughness of the FG and CG samples show a similar trend that the toughness is nearly a constant in the range of  $25\text{--}1100\ ^\circ\text{C}$ , but it declines fast over  $1100\ ^\circ\text{C}$ .

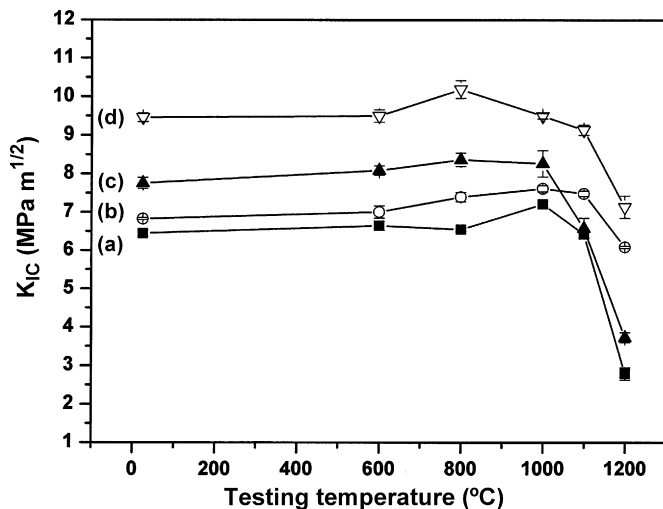


Fig. 7. The fracture toughness of FG  $\text{Ti}_3\text{Si}(\text{Al})\text{C}_2$  (a), CG  $\text{Ti}_3\text{Si}(\text{Al})\text{C}_2$  (b), FG  $\text{Ti}_3\text{AlC}_2$  (c), and CG  $\text{Ti}_3\text{AlC}_2$  (d) samples as a function of the testing temperatures.

#### 4. Discussion

Many works have been carried on to investigate the fracture toughness of  $\text{Ti}_3\text{SiC}_2$  and  $\text{Ti}_3\text{AlC}_2$  using different methods. The measured toughness of  $\text{Ti}_3\text{SiC}_2$  and  $\text{Ti}_3\text{AlC}_2$  with different impurity and/or sample size was summarized in Table 2. The measured  $K_{\text{IC}}$  of  $\text{Ti}_3\text{AlC}_2$  by Peng<sup>13</sup> is only  $4.6\ \text{MPa m}^{1/2}$ , which is ascribed to the effect of residual pores. Zhou et al.<sup>15</sup> found that the fracture toughness of  $\text{Ti}_3\text{AlC}_2$ , prepared by two different synthesized methods, was ranged from  $5.7$  to  $9.1\ \text{MPa m}^{1/2}$ . For full dense  $\text{Ti}_3\text{AlC}_2$  with different grain size in this work, the valid fracture toughness is about  $7.76\text{--}9.46\ \text{MPa m}^{1/2}$ , which is close to the reported  $K_{\text{IC}}$  value by Wang and Zhou.<sup>14</sup>

For  $\text{Ti}_3\text{SiC}_2$ , most of the reported  $K_{\text{IC}}$  values are within  $6\text{--}8\ \text{MPa m}^{1/2}$ . The measured toughness of  $\text{Ti}_3\text{SiC}_2$  by SEPB<sup>11</sup> and R-curve<sup>10,12</sup> may be overestimated due to the effect of sample size, the impurities, and a material's R-curve behavior.<sup>10,12,30</sup> Li et al.<sup>6</sup> reported that the  $K_{\text{IC}}$  of  $\text{Ti}_3\text{SiC}_2$  with the average grain length of  $11.3\ \mu\text{m}$  and grain width of  $2.3\ \mu\text{m}$  was only  $4.52\ \text{MPa m}^{1/2}$ , which might be the lowest reported toughness, but the reported flexural strength was also very low (about  $300\ \text{MPa}$ ). Recently, Bao and Zhou<sup>7</sup> have evaluated the fracture toughness of  $\text{Ti}_3\text{SiC}_2$  containing  $7\ \text{wt.}\%$  TiC using three different methods and the reported values are  $6.2\text{--}6.6\ \text{MPa m}^{1/2}$ . The fracture toughness measured by SEPB was the lowest due to the narrowest crack width, and the  $K_{\text{IC}}$  value of  $6.2\ \text{MPa m}^{1/2}$  could be considered as the reference toughness. In this work, the fracture toughness of  $\text{Ti}_3\text{Si}(\text{Al})\text{C}_2$  with similar grain sizes (FG samples) is  $6.45\ \text{MPa m}^{1/2}$ , which confirms the convenience and validity of the CNB method. It can also be found that the measured toughness by SENB is slightly higher than that by CNB or SEPB, as shown in Table 2. If the notch width is less than  $200\ \mu\text{m}$ , the measured toughness of  $\text{Ti}_3\text{Si}(\text{Al})\text{C}_2$  via the SENB method<sup>26</sup> is slightly higher than the reference toughness ( $6.2\ \text{MPa m}^{1/2}$ ). These results suggest that the measured toughness of  $\text{Ti}_3\text{SiC}_2$  by the traditional fracture toughness testing method, i.e. the SENB method, is reliable when the notch width is less than  $200\ \mu\text{m}$ . Gilbert et al.<sup>10,12</sup> investigated the effect of grain size on the fracture toughness of  $\text{Ti}_3\text{SiC}_2$  and found that the toughness of the CG samples was higher than that of the FG specimens, which was in good agreement with our results. In addition, these results indicate that the SENB, CNB, and SEPB methods are all suitable to determine the fracture toughness of MAX phases when an appropriate notch width (below a critical notch width) is introduced. Considering the scatter of the measured toughness of  $\text{Ti}_3\text{Si}(\text{Al})\text{C}_2$  and  $\text{Ti}_3\text{AlC}_2$  showing in Table 2, the SEPB and CNB methods seem to be more reliable.

Our results demonstrate that  $\text{Ti}_3\text{Si}(\text{Al})\text{C}_2$  and  $\text{Ti}_3\text{AlC}_2$  have a relatively high fracture toughness ( $>6.4\ \text{MPa m}^{1/2}$ ). This phenomenon can be explained according to the following facts. (1) The fracture toughness is a property related to energy absorption. The energy absorbing mechanism has been widely investigated for  $\text{Ti}_3\text{SiC}_2$  and  $\text{Ti}_3\text{AlC}_2$  including basal plane slip, grain buckling, crack deflection, crack branching, pull-out, and delamination of the laminated grains.<sup>1,4,5,31</sup> (2) The

Table 2  
Summary of the measured fracture toughness of  $\text{Ti}_3\text{SiC}_2$  and  $\text{Ti}_3\text{AlC}_2$  at room temperature using different methods

Samples	Sample size ( $\text{mm}^3$ )	Testing method	Fracture toughness ( $\text{MPa}\cdot\text{m}^{1/2}$ )	Ref.
$\text{Ti}_3\text{SiC}_2$ (<3 vol.% TiC)	$2 \times 3 \times 24$	SENB <sup>a</sup>	$4.52 \pm 0.15$	6
$\text{Ti}_3\text{SiC}_2$ (7 wt.% TiC)	$4 \times 8 \times 36$	SEPB <sup>b</sup>	$6.2 \pm 0.32$	7
		CNB <sup>a</sup>	$6.6 \pm 0.15$	
		SENB <sup>b</sup>	$6.62 \pm 0.12$	
$\text{Ti}_3\text{SiC}_2$ (TiC)	$2 \times 4 \times 24$	SENB <sup>b</sup>	7.20	8
$\text{Ti}_3\text{SiC}_2$ (7 wt.% TiC)	$3 \times 6 \times 36$	SENB <sup>b</sup>	7.88	9
$\text{Ti}_3\text{SiC}_2$ (3 vol.% TiC)	$3 \times 4 \times 18$	SEPB <sup>b</sup>	11.2	11
$\text{Ti}_3\text{SiC}_2$ (2 vol.% SiC)	2.9 mm thick $\times$ 19 mm wide compact-tension specimens	R-curve	9.5 (FG)	10,12
			16 (CG)	
$\text{Ti}_3\text{Si(Al)C}_2$	$4 \times 8 \times 36$	SENB <sup>b</sup>	6.80	26
$\text{Ti}_3\text{Si(Al)C}_2$	$3 \times 4 \times 36$	CNB <sup>a</sup>	$6.45 \pm 0.09$ (FG)	This work
			$6.83 \pm 0.03$ (CG)	
$\text{Ti}_3\text{AlC}_2$ (TiC)	$3 \times 6 \times 36$	SENB <sup>b</sup>	$4.6 \pm 0.3$	13
$\text{Ti}_3\text{AlC}_2$	$4 \times 8 \times 36$	SENB <sup>b</sup>	7.2	14
$\text{Ti}_3\text{AlC}_2$ ( $\text{Ti}_2\text{AlC}$ , TiC)	$4 \times 6 \times 35$	SENB <sup>b</sup>	$5.7 \pm 0.3$ (HPed)	15
			$9.1 \pm 0.3$ (SHS-SPSed)	
$\text{Ti}_3\text{AlC}_2$	$3 \times 4 \times 36$	CNB <sup>a</sup>	$7.76 \pm 0.14$ (FG)	This work
			$9.46 \pm 0.11$ (CG)	

HPed = hot-pressed and SHS-SPSed = self propagating high-temperature synthesis-spark plasma sintered.

<sup>a</sup> Four-point bending tests.

<sup>b</sup> Three-point bending tests.

capacity of absorbing energy will become stronger for CG samples because of the larger grain size. Thus,  $\text{Ti}_3\text{Si(Al)C}_2$  and  $\text{Ti}_3\text{AlC}_2$  have a relatively high fracture toughness (above  $6.4 \text{ MPa}\cdot\text{m}^{1/2}$ ) and the measured toughness of the CG specimens are higher than that of the FG samples at all testing temperatures.

The high-temperature fracture toughness of  $\text{Ti}_3\text{SiC}_2$  has been reported to be practically constant when the testing temperature is before the ductile–brittle transition temperature (DBTT) and then decreases rapidly.<sup>6,26</sup> In this work, a similar trend was found for  $\text{Ti}_3\text{Si(Al)C}_2$  and  $\text{Ti}_3\text{AlC}_2$ . It should be pointed out that the measured fracture toughness of  $\text{Ti}_3\text{Si(Al)C}_2$  and  $\text{Ti}_3\text{AlC}_2$  above DBTT will lose its validity because the stress distribution is no longer elastic during the testing. Since  $\text{Ti}_3\text{Si(Al)C}_2$  and  $\text{Ti}_3\text{AlC}_2$  are promising structural components, it is necessary and helpful to investigate the fracture toughness above DBTT for the design and application of these two ceramics. The mechanism for the degradation of the fracture toughness is mainly ascribed to the decline of elastic modulus at temperatures above DBTT.<sup>6,7,26</sup> Careful analysis of the change of the fracture toughness from room temperature to  $1100^\circ\text{C}$  (Fig. 6), it can be found that the measured toughness is slightly increased with increasing temperature. This phenomenon has been found in measuring the toughness by the SENB method in our previous work.<sup>26</sup> The reason for the increment of the toughness of  $\text{Ti}_3\text{Si(Al)C}_2$  and  $\text{Ti}_3\text{AlC}_2$  should be related to the closing up of flaws at the tip of the notch at high temperatures. This effect seems to be more obvious for measuring the toughness of  $\text{Ti}_3\text{Si(Al)C}_2$ , which is imputed to the poor oxidation resistance of  $\text{Ti}_3\text{Si(Al)C}_2$  compared with  $\text{Ti}_3\text{AlC}_2$ . Further work is needed to show light on it.

## 5. Conclusions

The effects of grain size, notch width, and testing temperature on the fracture toughness of  $\text{Ti}_3\text{Si(Al)C}_2$  and  $\text{Ti}_3\text{AlC}_2$ , were investigated using the chevron-notched beam (CNB) method. The measured toughness was ranged from 6.4 to  $7.2 \text{ MPa}\cdot\text{m}^{1/2}$  for  $\text{Ti}_3\text{Si(Al)C}_2$  and 7.6 to  $10.2 \text{ MPa}\cdot\text{m}^{1/2}$  for  $\text{Ti}_3\text{AlC}_2$  with limited standard deviation scatters. For a fixed notch width and testing temperature, the fracture toughness of coarse-grained (CG) samples is higher than that of fine-grained (FG) samples.

Notch width has great effect on the measured toughness of  $\text{Ti}_3\text{Si(Al)C}_2$  and  $\text{Ti}_3\text{AlC}_2$  using the CNB method. The critical notch width for valid  $K_{IC}$  measurements of this kind of quasi-plastic ceramic is about  $250 \mu\text{m}$ .

The high-temperature toughness of  $\text{Ti}_3\text{Si(Al)C}_2$  and  $\text{Ti}_3\text{AlC}_2$  with different grain sizes are insensitive to the testing temperatures before the brittle–ductile transition temperature (DBTT) (about  $1100^\circ\text{C}$ ), but it declines fast over  $1100^\circ\text{C}$ . The degradation of the fracture toughness is mainly imputed to the decline of elastic modulus at temperatures above DBTT.

## Acknowledgements

This work was supported by the National Outstanding Young Scientist Foundation (No. 59925208 for Y.C. Zhou, No. 50125204 for Y.W. Bao), Natural Sciences Foundation of China under Grant Nos. 50232040, 50302011, 90403027, ‘863’ project, High-tech Bureau of the Chinese Academy of Sciences, and French Atomic Energy Commission.

## References

- Zhou, Y. C. and Sun, Z. M., Microstructure and mechanism of damage tolerance for  $\text{Ti}_3\text{SiC}_2$  bulk ceramics. *Mater. Res. Innovations*, 1999, **2**, 360–363.
- Barsoum, M. W. and El-Raghy, T., Synthesis and characterization of a remarkable ceramic:  $\text{Ti}_3\text{SiC}_2$ . *J. Am. Ceram. Soc.*, 1996, **79**, 1953–1956.
- Sun, Z. M., Zhou, Y. C. and Li, M. S., High temperature oxidation behavior of  $\text{Ti}_3\text{SiC}_2$ -based material in air. *Acta Mater.*, 2001, **49**(20), 4347–4353.
- Barsoum, M. W., The  $\text{M}_{N+1}\text{AX}_N$  phases: a new class of solids; thermodynamically stable nanolaminates. *Prog. Solid. Chem.*, 2000, **28**, 201–281.
- Low, I. M., Lee, S. K. and Lawn, B. R., Contact damage accumulation in  $\text{Ti}_3\text{SiC}_2$ . *J. Am. Ceram. Soc.*, 1998, **81**, 225–228.
- Li, J. F., Pan, W., Sato, F. and Watanabe, R., Mechanical properties of polycrystalline  $\text{Ti}_3\text{SiC}_2$  at ambient and elevated temperatures. *Acta Mater.*, 2001, **49**, 937–945.
- Bao, Y. W. and Zhou, Y. C., Effect of sample size and testing temperature on the fracture toughness of  $\text{Ti}_3\text{SiC}_2$ . *Mater. Res. Innovations*, 2005, **9**(2), 41–42.
- Li, S. B., Xie, J. X., Zhao, J. Q. and Zhang, L. T., Mechanical properties and mechanism of damage tolerance for  $\text{Ti}_3\text{SiC}_2$ . *Mater. Lett.*, 2002, **57**, 119–123.
- Zhou, Y. C., Sun, Z. M., Chen, S. Q. and Zhang, Y., In situ hot-pressing/solid–liquid reaction synthesis of dense titanium silicon carbide bulk ceramics. *Mater. Res. Innovations*, 1998, **2**, 142–146.
- Chen, D., Shirato, K., Barsoum, M. W., El-Raghy, T. and Ritchie, R. O., Cyclic fatigue-crack growth and fracture properties in  $\text{Ti}_3\text{SiC}_2$  ceramics at elevated temperatures. *J. Am. Ceram. Soc.*, 2001, **84**, 2914–2920.
- Gao, N. F., Miyamoto, Y. and Zhang, D., Dense  $\text{Ti}_3\text{SiC}_2$  prepared by reactive HIP. *J. Mater. Sci.*, 1999, **34**, 4385–4392.
- Gilbert, C. J., Bloyer, D. R., Barsoum, M. W., El-Raghy, T., Tomsia, A. P. and Ritchie, R. O., Fatigue-crack growth and fracture properties of coarse and fine-grained  $\text{Ti}_3\text{SiC}_2$ . *Scripta Mater.*, 2000, **42**, 761–767.
- Peng, L. M., Fabrication and properties of  $\text{Ti}_3\text{AlC}_2$  particulates reinforced copper composites. *Scripta Mater.*, 2007, **56**, 729–732.
- Wang, X. H. and Zhou, Y. C., Microstructure of properties of  $\text{Ti}_3\text{AlC}_2$  prepared by the solid–liquid reaction synthesis and simultaneous in situ hot pressing process. *Acta Mater.*, 2002, **50**(12), 3141–3149.
- Zhou, A. G., Wang, C. A. and Huang, Y., Synthesis and mechanical properties of  $\text{Ti}_3\text{AlC}_2$  by spark plasma sintering. *J. Mater. Sci.*, 2003, **38**(14), 3111–3115.
- Bao, Y. W. and Zhou, Y. C., A new method for precracking beam for fracture toughness experiments. *J. Am. Ceram. Soc.*, 2006, **89**, 1118–1121.
- Munz, D., Bubsey, R. T. and Shannon Jr., J. L., Fracture toughness determination of  $\text{Al}_2\text{O}_3$  using four-point-bend specimens with straight through and chevron notches. *J. Am. Ceram. Soc.*, 1980, **63**, 300–305.
- Mukhopadhyay, A. K., Datta, S. K. and Chakraborty, D., Fracture toughness of structural ceramics. *Ceram. Int.*, 1999, **25**, 447–454.
- Munz, D., Bubsey, R. T. and Srawley, J. E., Compliance and stress intensity coefficients for short bar specimens with chevron notches useful for fracture toughness testing of ceramics. *Int. J. Fract.*, 1980, **16**, 359–374.
- Munz, D., Bubsey, R. T. and Shannon Jr., J. L., Performance of chevron-notch short bar specimen in determining the fracture toughness of silicon nitride and aluminum oxide. *J. Test. Eval.*, 1980, **8**, 103–107.
- Munz, D., Shannon Jr., J. L. and Bubsey, R. T., Fracture toughness calculation from maximum load in four-point bend tests of chevron notch specimens. *Int. J. Fract.*, 1980, **16**, R137–R141.
- Mizuno, M. and Okuda, H., VAMAS round robin on fracture toughness of silicon nitride. *J. Am. Ceram. Soc.*, 1995, **78**, 1793–1801.
- ISO 24370. Fine Ceramics (advanced ceramics, advanced technical ceramics)–Test Method for Fracture Toughness of Monolithic Ceramics at Room Temperatures by Chevron Notched Beam (CNB) Method. International Organization for Standards, Geneva, 2005.
- Zhou, Y. C., Zhang, H. B., Li, M. S., Wang, J. Y. and Bao, Y. W., Preparation of TiC-free  $\text{Ti}_3\text{SiC}_2$  with improved oxidation resistance by substitution of Si with Al. *Mater. Res. Innovations*, 2004, **8**(2), 97–102.
- Zhang, H. B., Zhou, Y. C., Bao, Y. W. and Li, M. S., Improving the oxidation resistance of  $\text{Ti}_3\text{SiC}_2$  by forming a  $\text{Ti}_3\text{Si}_{0.9}\text{Al}_{0.1}\text{C}_2$  solid solution. *Acta Mater.*, 2004, **52**(12), 3631–3637.
- Zhou, Y. C., Wan, D. T., Bao, Y. W. and Wang, J. Y., In situ processing and high-temperature properties  $\text{Ti}_3\text{Si}(\text{Al})\text{C}_2/\text{SiC}$  composites. *Int. J. Appl. Ceram. Soc.*, 2006, **3**(1), 47–54.
- Wan, D. T., Zhou, Y. C., Bao, Y. W. and Yan, C. K., In situ reaction synthesis and characterization of  $\text{Ti}_3\text{Si}(\text{Al})\text{C}_2/\text{SiC}$  composites. *Ceram. Int.*, 2006, **32**(8), 883–890.
- Zhou, Y. C., Sun, Z. M. and Yu, B. H., Microstructure of  $\text{Ti}_3\text{SiC}_2$  prepared by the in situ hot processing/solid–liquid reaction process. *Z. Metallkd.*, 2000, **91**(11), 937–941.
- Salem, J. A., Ghosn, L., Jenkins, M. G. and Quinn, G. D., Stress intensity factor coefficients for chevron-notched flexure specimens and a comparison of fracture toughness methods. *Ceram. Eng. Sci. Proc.*, 1999, **20**(3), 503–512.
- Wang, H., Isgrò, G., Pallav, P., Feilzer, A. J. and Chao, Y. L., Influence of test methods on fracture toughness of a dental porcelain and a soda lime glass. *J. Am. Ceram. Soc.*, 2005, **88**, 2868–2873.
- El-Raghy, T., Zavaliangos, A., Barsoum, M. W. and Kalidindi, S. R., Damage mechanisms around hardness indentation in  $\text{Ti}_3\text{SiC}_2$ . *J. Am. Ceram. Soc.*, 1997, **80**, 513–516.